ORIGINAL PAPER

Distance-Based Detection of Ag$^+$ with Gold Nanoparticles-Coated Microfluidic Paper

Yu Zhang[1,2] · Yu-Long Li[1] · Shu-Hua Cui[3] · Cong-Ying Wen[1] · Peng Li[2] · Jian-Feng Yu[1] · Shi-Ming Tang[1] · Jing-Bin Zeng[1]

Abstract

In this study, we developed a microfluidic paper analysis device (μPAD) for distance-based detection of Ag$^+$ in water. The μPAD was manufactured by wax printing method on filter paper. Then, a layer of gold nanoparticles (AuNPs) was deposited and ascorbic acid was printed on the channel. In the detection, Ag$^+$ was reduced by ascorbic acid and coated on the surface of the AuNPs on the channel, forming Au@Ag core/shell nanoparticles. Based on the capillary flow principle, different concentrations of Ag$^+$ formed different distances of color ribbons. Thus, quantitative detection of Ag$^+$ can be achieved by measuring the distance of the color ribbon. The detection limit of this method was as low as 1 mg·L^{-1} within 15 min and the interference of common metal ions in water can be eliminated. In conclusion, this method had successfully realized the leap from colorimetry to direct reading, realizing fast read and easy manipulation with low-cost.

Keywords Ag$^+$ detection · Colorimetric detection · Distance-based detection · Microfluidic paper analysis device · AuNPs

1 Introduction

Ag$^+$ is a prevalent pollutant and highly toxic metal ion [1]. It will cause serious failures such as organ failure, mitochondrial damage and slow growth of children due to its bioaccumulation in food chain of human being. It is reported that when the content of Ag$^+$ in water exceeds 1.6 nM, it will have toxic effect on aquatic organisms and microorganisms [2]. The U.S. Environmental Protection Agency (EPA) has set the maximum level of Ag$^+$ in drinking water at 50 μg·L^{-1} (~ 460 nM)[3]. Therefore, it is necessary to establish a low-cost, fast and highly sensitive method for detecting Ag$^+$. To reach this goal, some physicochemical

---

Yu Zhang and Yu-Long Li contribute equally to this work.

✉ Cong-Ying Wen
    flcyxt@163.com

✉ Jing-Bin Zeng
    xmuzjb@163.com

1 College of Science, China University of Petroleum (East China), Qingdao 266580, China

2 College of Chemical Engineering, China University of Petroleum (East China), Qingdao 266580, China

3 Qingdao Customs Technology Center, Qingdao 266002, China

technologies including atomic absorption spectrometry, ICP atomic emission spectrometry, fluorescence spectrometry and electrochemical method have been employed to Ag$^+$ detection. Although these methods exhibit high detection sensitivity and reliability, they need sophisticated instruments and skilled technical staffs, which are unsuitable for on-site detection.

Recently, the development of microfluidic paper analysis device (μPAD) has aroused great excitement, which has been applied to food analysis, environmental monitoring and clinical diagnosis due to its advantages of simplicity, easy handling, low sample and reagent consumption, high accuracy and portability [4–7]. Moreover, multiple detection channels also can be made on a piece of paper to achieve simultaneous detection of multiple targets [8–11]. The μPAD detection principle was mainly based on the change of color and distance [12–14]. For the ones based on color change, it was difficult to achieve high visual resolution and high sensitivity because it was difficult to judge unobvious changes in color with naked eyes. To solve this problem, some researchers used images processing software to analyze the color change and connected them with mobile applications [15, 16]. For example, Mohammad et al. [17] developed a hand drawn paper-based optical assay plate for determination of Ag$^+$ in water by image analysis software, which improved the detection sensitivity, but it increased the complexity and detection

cost. While, the detection methods based on distance can judge the concentrations of analyte. Liu et al. [18] developed a disposable, instrument-free paper-based analytical device based on a paper strip inkjet-printed with CdTe QDs for the analysis of Ag^+. Without auxiliary instruments, these distance-based methods improved the detection accuracy, sensitivity and simplified manipulation [19–21].

So far, nanosensors based on gold nanoparticles (AuNPs) have been used as a simple and convenient platform for colorimetric analysis, with their unique Localized Surface Plasmon Resonance (LSPR) characteristics and nanoscale effects [22–24]. Researchers also applied AuNPs to detect Ag^+. Alizadeh et al. developed a colorimetric assay for Ag^+ detection based on mixed monolayers of 6-nitrohexane-1-thiol and octanethiol modified AuNPs. This method realized a visually and instrumentally detectable color change from pale-brown to dark blue due to aggregation of the AuNPs [25]. Liu et al. presented a new colorimetric sensor based on color change between AuNPs and Au@Ag core/shell nanoparticles (Au@Ag NPs), and it was successfully applied to the determination of Ag^+ in real samples[26].The colorimetric detection methods based on Au@Ag NPs had the characteristics of simple production, obvious color change and high selectivity, which facilitated fast detection and the immediate assessment of the sudden risk and danger [27, 28]. However, most of methods still suffered the disadvantages of low naked eye resolution and inconvenient operation.

In our previous work, we synthesized AuNPs and Au@Ag NPs, and developed a series of detection methods based on AuNPs and Au@Ag NPs [29, 30]. Herein, based on the previous work, a distance-based Ag^+ detection with the AuNPs-coated µPAD was developed (Scheme 1). The sample solution was dropped into the sample cell at the end of the test paper. Based on the capillary flow principle, the solution flowed along a predetermined channel, and the Ag^+ in the solution was reduced and coated on the surface of AuNPs during the flow process. After 15 min, an orange color ribbon would be formed on the surface of the test paper. The different distances of color ribbons were obtained with different concentrations of Ag^+. Thus, the concentration of Ag^+ in solution can be detected directly by measuring the distance of the color ribbon.

2 Experimental Section

2.1 Reagents and Instruments

Chloroauric acid ($HAuCl_4$) was purchased from Macklin, silver nitrate and anhydrous ethanol were purchased from Xilong Chemical Co., Ltd. Polyvinylpyrrolidone (PVP, MW: 10,000) was purchased from Aladdin. Iron (III) chloride hexahydrate, cupper (II) sulfate pentahydrate, anhydrous sodium sulfate, anhydrous potassium sulfate, nickel chloride, sodium citrate dihydrate and ascorbic acid were purchased from Sinopharm Chemical Reagent Co., Ltd. Drinking water was purchased from Wahaha Group Co., Ltd. Qualitative filter paper (Whatman Grade 1 NO. 1001-125) from Whatman TM was used to paper base. Heating plate (SB-1.8–4) was purchased from Longkou Xianke Instrument Co., Ltd. Inkjet Printers (L380) used to print ascorbic acid was purchased from Epson. Transmission electron microscopy (TEM) images were acquired by a JEM-1400 (JEOL) electron microscope. Scanning electron microscope (SEM) images were acquired by a S4800 electron microscope from Hitachi Corporation of Japan.

Scheme 1 Schematic diagram for the principle of distance-based Ag^+ detection with the AuNPs-coated µPAD
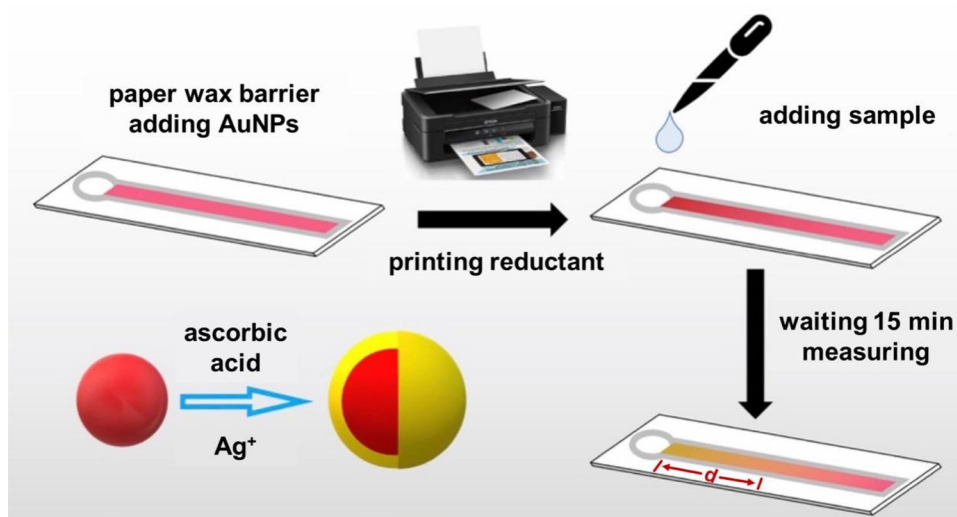
2.2 Synthesis of AuNPs

In a typical procedure, 5 mL of $HAuCl_4$ (0.02428 mol·L^{-1}) and 95 mL of H_2O were mixed in a three-neck flask and heated up to 400 °C under stirring. After boiling, freshly prepared sodium citrate dihydrate solution (0.1146 g of sodium citrate dihydrate was dissolved in 10 mL of water) was added into the three-neck flask, and the solution was continued to heat for 15 min. The solution initially showed a pale-yellow color of $HAuCl_4$, turned black quickly within 1 min, and finally stabilized to wine red. The three-necked flask containing the reaction liquid was quickly placed in cold water for cooling and stored at 4 °C.

2.3 Synthesis of Au@Ag NPs

1 mL of AuNPs and 1 mL of ascorbic acid (0.1 mol·L^{-1}) were mixed adequately. Then, 100 μL (0, 10, 25, 50, 100 mg·L^{-1}) of Ag$^+$ solutions were added, respectively. Finally, the solution was shacked well, stood for 2 min and stored at 4 °C.

2.4 Preparation of μPAD

Solid wax screen printing was used to make μPAD. As shown in Scheme 2, 9.5 cm apart parallel lines were drawn on a Whatman # (ø125 mm) filter paper, and the side was sealed completely with transparent tape. On the other side of the filter paper, 8 mm wide transparent tape was stuck on the predetermined area of filter paper by 9 mm interval. Paraffin wax was used to paint on the filter paper until a layer of visible thin paraffin wax was coated on the surface of the filter paper. After that, the filter paper was placed on the electric heating plate (65 °C). The paraffin wax on the filter paper would melt into the filter paper fiber, and then the filter paper was removed, leaving a hydrophilic channel in the filter paper. 0.1 g PVP was dissolved in 9 mL absolute ethanol completely. 1 mL of AuNP solution was slowly added to the PVP solution. The channel of filter paper was evenly wetted with the above AuNPs. The above operation was repeated 10

times. Finally, a layer of AuNPs was deposited in the channel. 4.4 g ascorbic acid was dissolved in 50 mL deionized water and added into ink-jet printer ink cartridge as ink [31, 32]. The filter paper was fixed in the predetermined printing position of A4 paper and printed 5 times in total. The transparent tape was pasted on the filter paper to prevent the solution from volatilizing during detection. A 9.5 cm test strip was obtained by cutting along the drawn parallel line. The sample cell was made with transparent tape at the end of test strip.

2.5 Detection of Ag$^+$ by μPAD

100 μL of sample was dropped into the sample cell. After reaction at room temperature for 15 min, a color ribbon was formed. The distance of the color ribbon was measured with a dividing rule.

3 Results and Discussion

3.1 Characterizations of AuNPs and Au@Ag NPs

The AuNPs were prepared by the Turkevich method [30, 33, 34]. As shown in Fig. 1, the as-synthesized AuNPs were spherical-like shapes with average diameters of 13 nm. AuNPs had the characteristics of uniform morphology and good dispersion.

The Au@Ag NPs were synthesized by reduction of Ag$^+$ using ascorbic acid on the surface of the AuNPs. As shown in Fig. 2a, after modification with Ag, the color of AuNP solution changed from red to orange, indicating that Ag$^+$ was reduced and successfully coated on the AuNPs. From the TEM image of the Au@Ag NPs (Fig. 2b), it could be clearly seen that the Au@Ag NPs had a core–shell structure. A layer of silver shell was evenly coated on the outer surface of central AuNPs. The diameter of Au@Ag NPs was about 21 nm, and the shape and size were uniform (Fig. 2c). Figure 2d was a selected area electron diffraction (SAED) pattern of a single Au@Ag particle. The HKL

Scheme 2 Schematic diagram for the manufacturing process of the AuNPs-coated μPAD
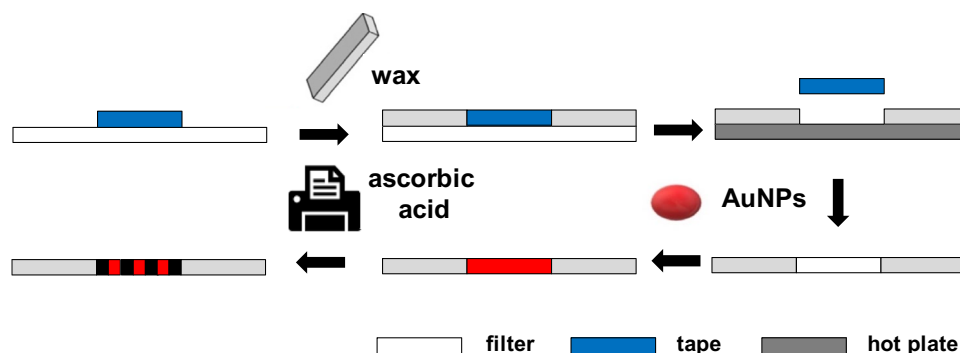
obtained from the calculation results corresponds to the face-centered cubic structure (Table 1). The (111), (200), (220), (311) and (331) crystal planes of Au or Ag indicated that the Au@Ag NPs were polycrystalline.

3.2 Characterization of µPAD

SEM and elemental analysis were performed on the prepared µPAD. Figure 3a showed a SEM image of the filter paper fiber and Fig. 3b was the image after magnifying it to 70,000

Fig. 1 a TEM image of AuNPs; **b** Particle size distribution histogram of AuNPs
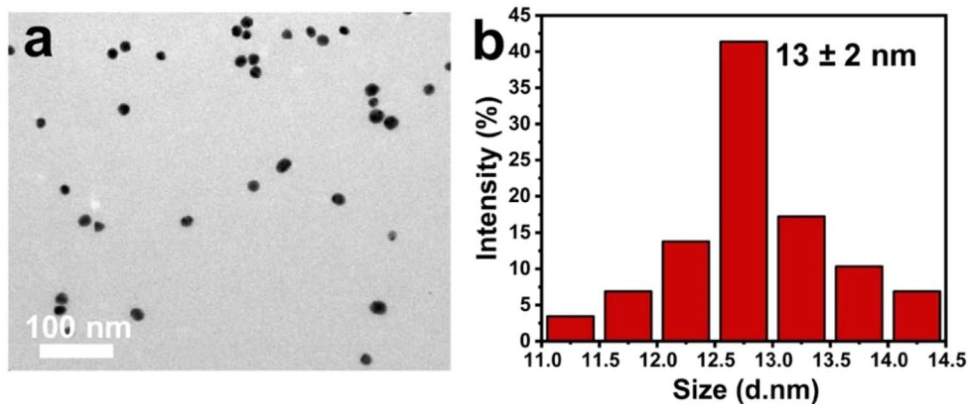
Fig. 2 a Color of Au@Ag NPs obtained using different concentrations of Ag^+. **b** TEM image of Au@Ag NPs (inset: a partial enlarged view of (b)). **c** Size distribution histogram of Au@Ag NPs. **d** an SAED pattern of Electron diffraction pattern of a single Au@Ag particle
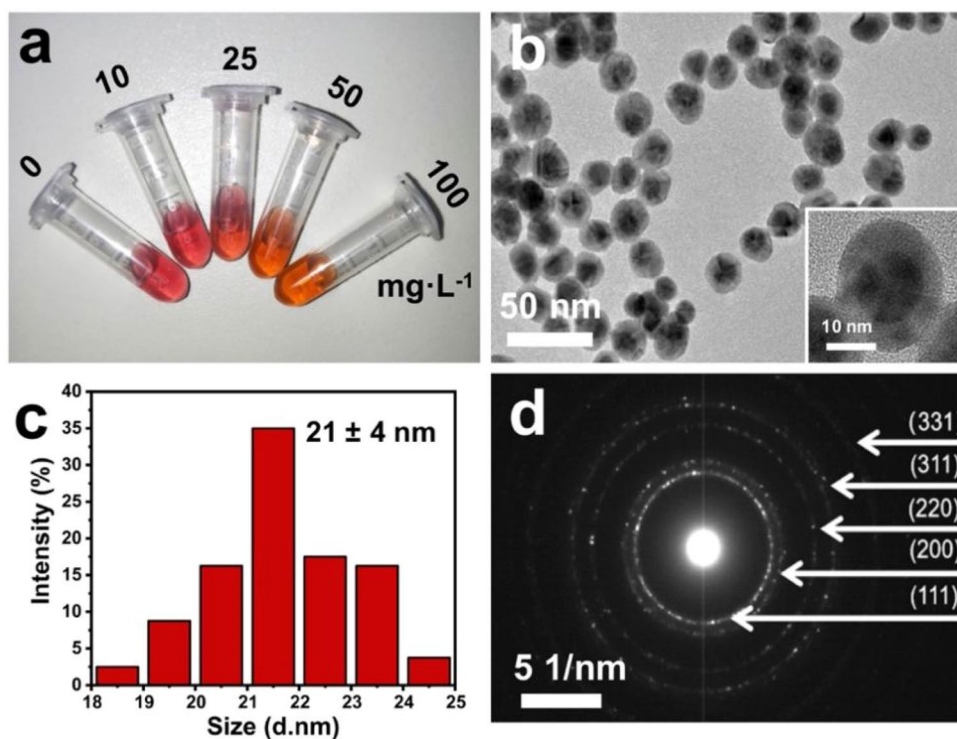
Table 1 The SAED pattern analysis results

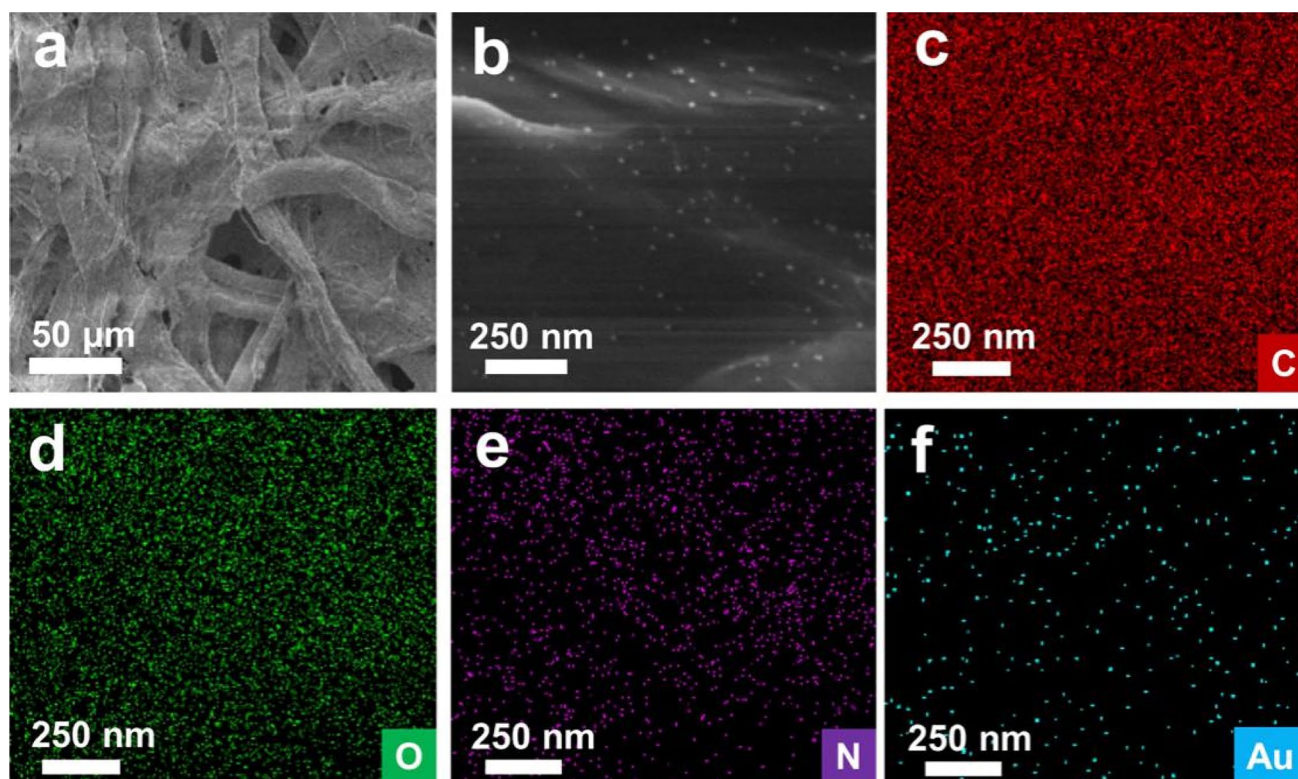| Diffraction ring number	R/mm	R^2	R^2_i/R^2_1	$(R^2_i/R^2_1) *3$	N	HKL
1	2.3	5.29	1.00	3.00	3	111
2	2.6	6.76	1.28	3.83	4	200
3	3.7	13.69	2.59	7.76	8	220
4	4.3	18.49	3.49	10.48	11	311
5	5.7	32.49	6.14	18.42	19	331

Fig. 3 Characterizations of the AuNPs-coated µPAD: **a** SEM image of the AuNPs-coated µPAD with 430 times magnification. **b** A partial enlarged view of (a). (**c~f**) SEM elemental maps of C, O, N, Au

times. It can be seen that there were many white bright spots on the fiber, which were AuNPs. It suggested that the AuNPs on the surface of filter paper did not agglomerate and had good dispersion. From Fig. 3c ~ f, the obvious distribution of C, O, N and Au can be seen. Among them, C, O and N were the main components of cellulose. The Au originating from AuNPs was relatively uniform, which further verified the reliability of the AuNPs deposition method in this study. It indicated that the deposited AuNPs had outstanding dispersion and stability, which was beneficial for the growth of Au@Ag NPs in subsequent experiments.

3.3 Detection of Ag⁺ by µPAD

The detection principle was that Ag^+ was reduced by ascorbic acid and wrapped on the surface of the AuNPs to form Au@Ag NPs during the flow process. Then, a color ribbon was obtained due to the capillary flow principle. Thus, the concentration of Ag^+ in solution can be detected directly by measuring the distance of the color ribbon. To demonstrate the feasibility of this method, SEM and elemental analysis were carried out after the reaction. Figure 4a was an image magnified 50,000 times, in which the dispersion of nanoparticles was relatively uniform. From the elemental maps of the particles (Fig. 4b, c), it can be found that the distribution

of Ag and Au were basically coincident, indicating that Au@Ag NPs were formed and the detection of Ag^+ can be realized with the µPAD.

For Ag^+ detection, the width of µPAD channel had a great influence on the experimental results, because the width of the channel affected the flow rate of the solution greatly, which affected the reaction rate of Ag^+ in the channel. In the experiment, 5 mm, 8 mm and 10 mm channel width were tried. Among them, the µPAD with 8 mm wide channel had the lowest detection limit, and the distance of the ribbon was longest (Fig. S1). Thus, an 8 mm wide channel was finally selected for the following experiments. Just as shown in Fig. 5a, the different distances of the color ribbons were formed by the different concentrations of Ag^+, and the detection limit was 1 mg·L⁻¹. The value of the distance was used to draw the detection calibration curve (Fig. 5b). The distance was positively correlated with the concentration of Ag^+. According to the calibration curve, the Ag^+ concentration of the sample can be easily read out by measuring the color ribbon. Moreover, the measurement deviation results were within 20% (Fig. 5c), indicating the method had good stability. In fact, Ag^+ itself can be reduced to Ag by ascorbic acid and a color ribbon was also obtained, which also can be applied to detect Ag^+. Thus, we carried out a control experiment, trying to print ascorbic acid directly instead of
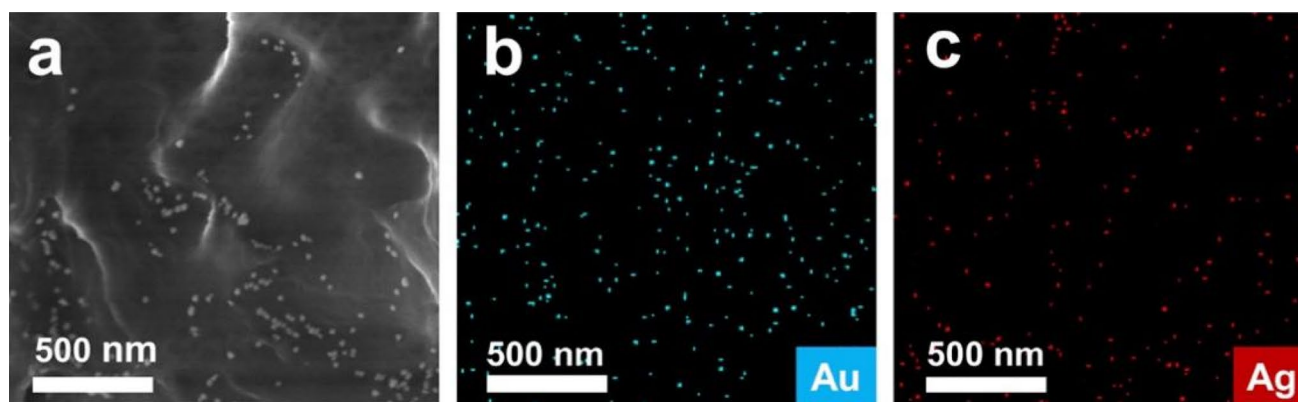
Fig. 4 Characterizations of µPAD after Ag^+ detection: (**a**) SEM image of µPAD after Ag^+ detection. **b** SEM elemental map of Au. **c** SEM elemental map of Ag
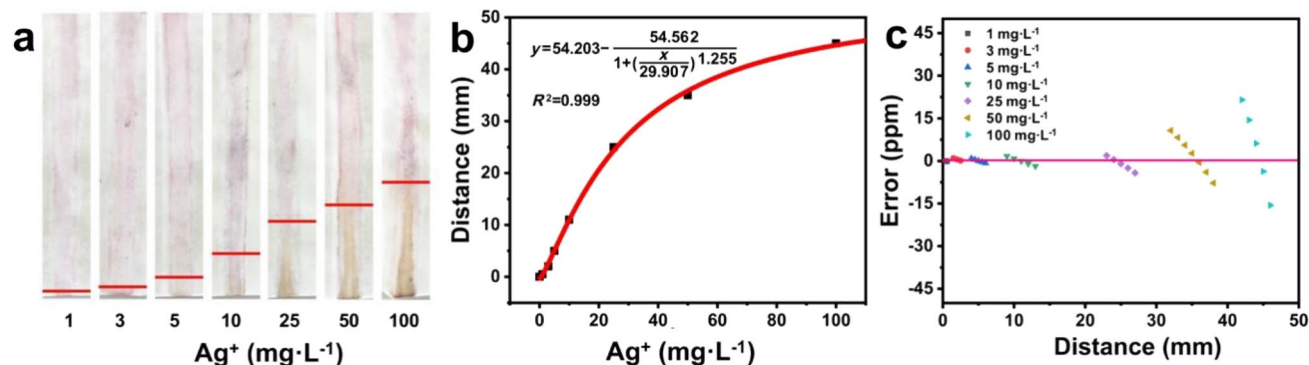

Fig. 5 **a** Picture of the µPAD after the detection of Ag^+. **b** Calibration curve of the µPAD after the detection of Ag^+. **c** Error analysis chart of the µPAD after the detection of Ag^+

depositing AuNPs on the surface of paper, and used it to detect Ag^+. As shown in Fig. S2, it can be seen that the µPAD without AuNPs had low sensitivity (50 mg·L^{-1}), and the color was dark compared with Fig. 5a. The reason for the dark color should be the existence of elemental silver alone. Therefore, it can be proved that the addition of AuNPs can greatly improve the detection ability of µPAD.

3.4 Anti-interference Investigation and Application of µPAD

Ag^+ detection in the real environment will be accompanied by a variety of interferences. The common interferences are the coexisting ions in water, such as Fe^{3+}, Cu^{2+}, Na^+, K^+, Ni^{2+}, and so on. Among them, Fe^{3+} and Cu^{2+} had the greatest impact on the detection of Ag^+. Fe^{3+} is easy to hydrolyze to form $Fe(OH)_3$, which affects measuring the distance. The potential of Cu^{2+} is similar to that of Ag^+, which may also be reduced by ascorbic acid. For Fe^{3+}, 0, 50 and 100 mg·L^{-1} Fe^{3+} were treated by the paper base

and the µPAD respectively. As shown in Fig. 6a, when the concentration of Fe^{3+} was 100 mg·L^{-1}, a yellow color ribbon was produced on the channel, which was attributed to the hydrolysis of Fe^{3+} to $Fe(OH)_3$. When the concentration of Fe^{3+} was 50 mg·L^{-1}, the yellow color ribbon was not obvious and similar to that of 0 mg·L^{-1} of Fe^{3+}. Thus, the concentration of Fe^{3+} should not exceed 50 mg·L^{-1} in the process of Ag^+ detection. 0, 200 and 500 mg·L^{-1} of Cu^{2+} mixed with 100 mg·L^{-1} of Ag^+ were detected respectively on the paper base and the µPAD respectively. It can be seen from Fig. 6b that Cu^{2+} did not form ribbons on the channel of common paper base. It showed that Cu^{2+} did not hydrolyze on the channel, which was not similar to Fe^{3+}. But, when the concentration of Cu^{2+} was 500 mg·L^{-1}, dark color ribbon appeared in the channel of µPAD. However, when the concentration of Cu^{2+} was 200 mg·L^{-1}, the color ribbon was similar to that of 0 mg·L^{-1} of Cu^{2+}, showing that the concentration of Cu^{2+} should not exceed 200 mg·L^{-1} in the process of Ag^+

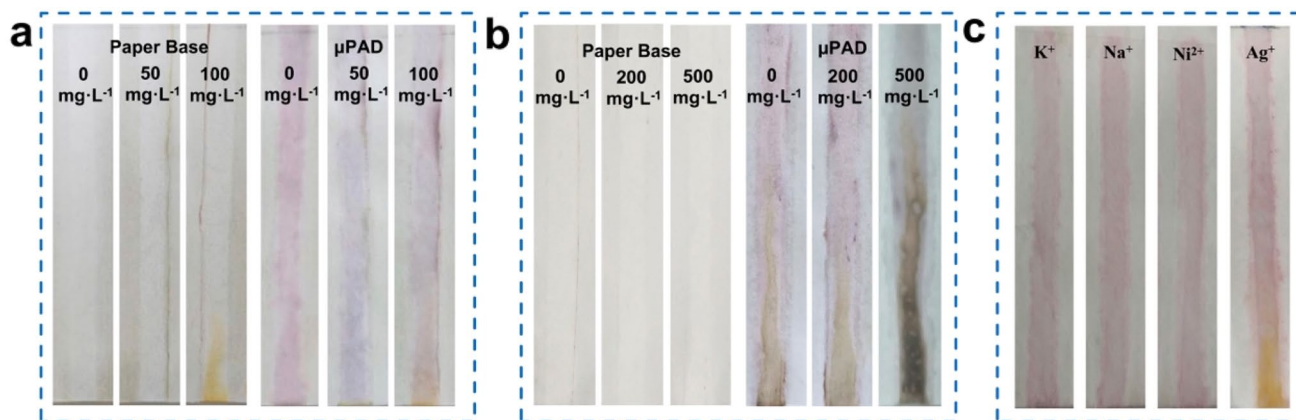**Fig. 6** **a** Fe^{3+} interference investigation on common paper base and the µPAD (left to right: 0, 50, 100 mg·L^{-1} Fe^{3+}). **b** Cu^{2+} interference investigation on common paper base and the µPAD. (left to right: 0, 200, 500 mg·L^{-1} Cu^{2+} mixed with 100 mg·L^{-1} Ag^{+}). **c** K^{+}, Na^{+}, Ni^{2+} interference investigations on the µPAD (K^{+}, Na^{+}, Ni^{2+}: 100 mg·L^{-1}, Ag^{+}: 25 mg·L^{-1})

Table 2 Detection results of recovery of Ag^{+} in drinking water samples

Added/ (mg·L^{-1})	Found/ (mg·L^{-1})	Recovery/%
25	23.4	93.6
50	47.9	95.8
100	104.8	104.8

detection. It can be seen from Fig. 6c that other common ions did not form ribbons in the channel of µPAD.

To evaluate the practicability of this detection method, we implemented this method in real water samples (drinking water). The drinking water samples were spiked with 25, 50, and 100 mg·L^{-1} of Ag^{+} (Table 2). The detection concentrations of this method were 23.4, 47.9 and 104.8 mg·L^{-1} with the recoveries of 93.6–104.8%, respectively, indicating that the proposed colorimetric assay has high accuracy.

4 Conclusion

In summary, we proposed a rapid, sensitive, low-cost µPAD platform coated AuNPs for distance-based detection of Ag^{+} in water. Ag^{+} can be reduced by ascorbic acid and coated on AuNPs to produce Au@Ag core/shell nanostructures appearing the color ribbon in the µPAD. Quantitative detection of Ag^{+} can be achieved by measuring the distance of the color ribbon. Only 15 min was needed in whole detection process and 1 mg·L^{-1} of Ag^{+} can be detected. The relative deviations of detection results were controlled within 20%. Moreover, the µPAD can resist the interference of the ions coexisting with Ag^{+} in water. Compared with traditional colorimetric methods, this method improved the detection sensitivity and realized easy manipulation. It is suitable for on-site and real-time analyses and can be used for reference in the following similar experiments.

References

1. Peng CF, Zhang YY, Wang LY, Jin ZY, Shao G. Colorimetric assay for the simultaneous detection of Hg^{2+} and Ag^{+} based on inhibiting the peroxidase-like activity of core–shell Au@Pt nanoparticles. Anal Methods. 2017;9(30):4363–70. https://doi.org/10.1039/c7ay01317e.
2. Hao C, Xua L, Xing C, Kuang H, Wang L, Xu C. Oligonucleotide-based fluorogenic sensor for simultaneous detection of heavy metal ions. Biosens Bioelectron. 2012;36(1):174–8. https://doi.org/10.1016/j.bios.2012.04.008.
3. Lin CY, Yu CJ, Lin YH, Tseng WL. Colorimetric sensing of silver(I) and mercury(II) ions based on an assembly of tween 20-stabilized gold nanoparticles. Anal Chem. 2010;82:8.
4. Chaiyo S, Apiluk A, Siangproh W, Chailapakul O. High sensitivity and specificity simultaneous determination of lead, cadmium and copper using µPAD with dual electrochemical and colorimetric detection. Sensors Actu B Chem. 2016;233:540–9. https://doi.org/10.1016/j.snb.2016.04.109.
5. Gaines M, Gonzalez-Guerrero MJ, Uchida K, Gomez FA. A microfluidic glucose sensor incorporating a novel thread-based electrode system. Electrophoresis. 2018;39(16):2131–5. https://doi.org/10.1002/elps.201800010.
6. Xiao W, Gao Y, Zhang Y, Li J, Liu Z, Nie J, Li J. Enhanced 3D paper-based devices with a personal glucose meter for

highly sensitive and portable biosensing of silver ion. Biosens Bioelectron. 2019;137:154–60. https://doi.org/10.1016/j.bios.2019.05.003.

7. Li H, Lin H, Lv W, Gai P, Li F. Equipment-free and visual detection of multiple biomarkers via an aggregation induced emission luminogen-based paper biosensor. Biosens Bioelectron. 2020;165:112336. https://doi.org/10.1016/j.bios.2020.112336.

8. Mentele MM, Cunningham J, Koehler K, Volckens J, Henry CS. Microfluidic paper-based analytical device for particulate metals. Anal Chem. 2012;84(10):4474–80. https://doi.org/10.1021/ac300309c.

9. Rattanarat P, Dungchai W, Cate D, Volckens J, Chailapakul O, Henry CS. Multilayer paper-based device for colorimetric and electrochemical quantification of metals. Anal Chem. 2014;86(7):3555–62. https://doi.org/10.1021/ac5000224.

10. Huangfu C, Zhang Y, Jang M, Feng L. A μPAD for simultaneous monitoring of Cu^{2+}, Fe^{2+} and free chlorine in drinking water. Sensors Actu B Chem. 2019;293:350–6. https://doi.org/10.1016/j.snb.2019.02.092.

11. Mensah ST, Gonzalez Y, Calvo-Marzal P, Chumbimuni-Torres KY. Nanomolar detection limits of Cd^{2+}, Ag^+, and K^+ using paper-strip ion-selective electrodes. Anal Chem. 2014;86(15):7269–73. https://doi.org/10.1021/ac501470p.

12. Gerold CT, Bakker E, Henry CS. Selective distance-based K^+ quantification on paper-based microfluidics. Anal Chem. 2018;90(7):4894–900. https://doi.org/10.1021/acs.analchem.8b00559.

13. Huang L, Wang J, Wang Q, Tang D, Lin Y. Distance-dependent visual fluorescence immunoassay on CdTe quantum dot-impregnated paper through silver ion-exchange reaction. Mikrochim Acta. 2020;187(10):563. https://doi.org/10.1007/s00604-020-04546-7.

14. Pratiwi R, Nguyen MP, Ibrahim S, Yoshioka N, Henry CS, Tjahjono DH. A selective distance-based paper analytical device for copper(II) determination using a porphyrin derivative. Talanta. 2017;174:493–9. https://doi.org/10.1016/j.talanta.2017.06.041.

15. Narang J, Singhal C, Mathur A, Dubey AK, Krishna Pn A, Anil A, Pundir CS, Naked-eye quantitative assay on paper device for date rape drug sensing via smart phone APP. Vacuu. 2018;153:300–5. https://doi.org/10.1016/j.vacuum.2018.03.056.

16. Vidal E, Lorenzetti AS, Lista AG, Domini CE. Micropaper-based analytical device (μPAD) for the simultaneous determination of nitrite and fluoride using a smartphone. Microchem J. 2018;143:467–73. https://doi.org/10.1016/j.microc.2018.08.042.

17. Dhavamani J, Mujawar LH, El-Shahawi MS. Hand drawn paper-based optical assay plate for rapid and trace level determination of Ag^+ in water. Sensors Actu B Chem. 2018;258:321–30. https://doi.org/10.1016/j.snb.2017.11.111.

18. Liu Q, Lin Y, Xiong J, Wu L, Hou X, Xu K, Zheng C. Disposable paper-based analytical device for visual speciation analysis of Ag(I) and silver nanoparticles (AgNPs). Anal Chem. 2019;91(5):3359–66. https://doi.org/10.1021/acs.analchem.8b04609.

19. Kim J-Y, Yeo M-K. A fabricated microfluidic paper-based analytical device (μPAD) for in situ rapid colorimetric detection of microorganisms in environmental water samples. Mole Cell Toxicol. 2016;12(1):101–9. https://doi.org/10.1007/s13273-016-0013-2.

20. Cai L, Ouyang Z, Song J, Yang L. Indicator-free argentometric titration for distance-based detection of chloride using microfluidic paper-based analytical devices. ACS Omega. 2020;5(30):18935–40. https://doi.org/10.1021/acsomega.0c02143.

21. Shibata H, Hiruta Y, Citterio D. Fully inkjet-printed distance-based paper microfluidic devices for colorimetric calcium determination using ion-selective optodes. Analyst. 2019;144(4):1178–86. https://doi.org/10.1039/c8an02146e.

22. Du J, Du H, Ge H, Fan J, Peng X. A plasmonic nano-sensor for the fast detection of Ag^+ based on synergistic coordination-inspired gold nanoparticle. Sensors Actu B Chem. 2018;255:808–13. https://doi.org/10.1016/j.snb.2017.08.034.

23. Martínez-Hernández ME, Goicoechea J, Arregui FJ. Hg^{2+} optical fiber sensor based on LSPR generated by gold nanoparticles embedded in LBL nano-assembled coatings. Sensors-basel. 2019;19(22):123. https://doi.org/10.3390/s19224906.

24. Dutta S, Saikia K, Nath P. Smartphone based LSPR sensing platform for bio-conjugation detection and quantification. RSC Adv. 2016;6(26):21871–80. https://doi.org/10.1039/c6ra01113f.

25. Alizadeh A, Abdi G, Khodaei MM. Colorimetric and visual detection of silver(I) using gold nanoparticles modified with furfuryl alcohol. Microchim Acta. 2016;183(6):1995–2003. https://doi.org/10.1007/s00604-016-1830-7.

26. Liu Y, Dai J, Xu L, Liu X, Liu J, Li G. Red to brown to green colorimetric detection of Ag^+ based on the formation of Au-Ag core-shell NPs stabilized by a multi-sulfhydryl functionalized hyperbranched polymer. Sensors Actu B Chem. 2016;237:216–23. https://doi.org/10.1016/j.snb.2016.06.096.

27. Zhao L, Wang Y, Li Z, Deng Y, Zhao X, Xia Y. Facile synthesis of chitosan-gold nanocomposite and its application for exclusively sensitive detection of Ag^+ ions. Carbohyd Polym. 2019;2:226. https://doi.org/10.1016/j.carbpol.2019.115290.

28. Bian J, Xia Y, Sang L, Zhu C, Li Y, Li G, Liu X, Wang X, Liu Y. A recyclable colorimetric probe: in situ fabrication of highly stable HPEI–AuNPs for selective Ag^+ detection. New J Chem. 2020;44(14):5438–47. https://doi.org/10.1039/d0nj00497a.

29. Zeng JB, Fan SG, Zhao CY, Wang QR, Zhou TY, Chen X, Yan ZF, Li YP, Xing W, Wang XD. A colorimetric agarose gel for formaldehyde measurement based on nanotechnology involving Tollens reaction. Chem Commun (Camb). 2014;50(60):8121–3. https://doi.org/10.1039/c4cc00914b.

30. Yiran L, Wang Q, Zhou X, Wen C-Y, Yu J, Han X, Li X, Yan Z, Zeng J. A convenient colorimetric method for sensitive and specific detection of cyanide using Ag@Au core–shell nanoparticles. Sensors Actu B Chem. 2016;228:366–72. https://doi.org/10.1016/j.snb.2016.01.022.

31. Younas M, Maryam A, Khan M, Nawaz AA, Jaffery SHI, Anwar MN, Ali L. Parametric analysis of wax printing technique for fabricating microfluidic paper-based analytic devices (μPAD) for milk adulteration analysis. Microfluid Nanofluid. 2019;23(3):9. https://doi.org/10.1007/s10404-019-2208-z.

32. Zhang H, Smith E, Zhang W, Zhou A. Inkjet printed microfluidic paper-based analytical device (μPAD) for glucose colorimetric detection in artificial urine. Biomed Microdev. 2019;21(3):48. https://doi.org/10.1007/s10544-019-0388-7.

33. Enustun BVTJ. Coagulation of colloidal gold. J Am Chem Soc. 1963;85(21):12.

34. Kimling J, Okenve B, Kotaidis V, Ballot H, Plech A. Turkevich method for gold nanoparticle synthesis revisited. J Physical Chem B. 2006;110(32):8.